Digital Edge Detection Based Pneumonia Detection in Chest Radiographs

Rahul Gowtham Poola [1*], Prema Teja Kommineni[2], Lahari P.L[3], and *Siva Sankar* Yellampalli[4]

[1]Department of Electronics and Communication Engineering, SRM University, Andhra Pradesh, India
[2]Department of Electronics and Communication Engineering, SRM University, Andhra Pradesh, India
[3]Department of Electronics and Communication Engineering, SRM University, Andhra Pradesh, India
[4]Department of Electronics and Communication Engineering, SRM University, Andhra Pradesh, India

Abstract. In response to the demand of pneumonia diagnosis, a digital detection algorithm utilizing chest X-ray images has been proposed. Despite this, X-ray images have the tendency of noise and spatial aliasing that tend to cause blurring of some boundaries, thus the importance of having a better edge detection algorithm is more warranted. The article presents a SIMULINK-based model for the process of edge detection, testing the performance of Canny, Laplacian of Gaussian, Prewitt, Sobel and Robert algorithms and most importantly their simulated results. Since some of the X rays are suspected to be afflicted by pneumonia, the radiographs are also converted into string numbers based on the features extracted as the X-ray's area of interest. One of the basic processes in image processing is the quality assessment of images, this work advocates for the inclusion of the objective criteria for the evaluation of the segmented images. Some performance evaluation metrics for various edge detection models are given and the relationships showed that the bacterial pneumonia affliction X rays have feature string values under 100 whereas the non-bacterial pneumonia X rays have values above 100.

1 Introduction

With pneumonia being one of the conditions with a high mortality rate, its radiological diagnosis through chest X-ray imaging is crucial in clinical practice, as its prompt and accurate identification contributes to proper management [1]. Research has indicated that advanced computer algorithms specifically, deep learning, an area of artificial intelligence, can aid in increasing the accuracy of detecting pneumonia in X-ray images of the chest [1]. Such progress is vital considering the fact that the visual signs of pneumonia are often insidious and heterogeneous making the manual reading of such images prone to overreliance on expertise unduly. Interestingly, while models like VGG-16, ResNet-50 and DenseNet-121 have reported a high accuracy in diagnosing diseases, Vision Transformer architecture has outperformed the former models in both embedding global context and capturing spatial relationships in chest X-ray images [2][3]. The accuracy has also improved with models that combine medical history with chest X-ray images, making it more applicable to actual practice [4]. Nonetheless, it is important to stress that despite such advances, the acquisition of large and heterogeneous datasets for training and subsequent testing in the real world still poses problems. Such developments point to the future where automated systems driven by artificial intelligence will improve the representation of patients while also reducing the costs associated with X-ray analysis [5].

CT scans are mostly performed with patients showing serious lung symptoms with respect to the factual understanding of the condition [6]. X-rays are basically a modality that catch visual pictures of the body parts by subjecting a small area of the body through ionizing radiation in a controlled regime. These pictures help the physician in the diagnosis and management of other medical conditions. It is also important to discriminate the Region of Interest that is being captured, from the background noise, and the artifacts present on the images. The Chest X-Ray (CXR) images which are the subject of this study tend to have a lot of background noise and wires making it difficult to detect the lesions that are infectively caused by Coronavirus. As a result, the image processing techniques are applied to eliminate irrelevant elements and sharpen the image. This work provides a review of the performance of diverse methodologies for diagnosing Pneumonia X-rays focusing on the X-ray images. The X-ray images thus created are manipulated using image processing techniques like feature extraction, filtering, noise reduction, edge detection and others through different algorithms and models.

Edge detection is one of the most important methods used when imaging objects to establish a boundary around them, in this case, it relies on the brightness level [7]. Similarly, a range of algorithms are incorporated for presuming edge features such as the Sobel, Robert, Prewitt, Laplacian of Gaussian (Log), and Canny's Method [8]. When images are analyzed, those

* Corresponding author: rahulgowtham_poola@srmap.edu.in

algorithms can produce specific features that stand out because of the edges that can be found in the image. Typically, edges represent local shifts or transitions in the image and can be located at the interface of two dissimilar regions within the image. In this respect, edges are critical in digital image processing tasks [9][10]. Many of edge detection has been put forward by researchers in the past; however, such pioneer works as Robert, Prewitt, and Sobel could be classified as early stage in focus gradient edge detectors, but with the addition of possession to noise and not able to create edges with strong definition [11]. Furthermore, the Laplacian operators are also known to have issues with fringing that can also be pronounced with curvature about the edges with a potential for severe localization issues. Canny however came up with a 4-stage process of edge detection algorithms which has generally proven to be one of the most preferred techniques for images with noise. Canny provides an edge detection algorithm that has a high probability of detection for definite edges while cutting down the possibility of false edge detection [12].

2 Proposed Methodology

The proposed model is using X-Ray images for pneumonia detection. The dataset used to test this proposed model in detecting pneumonia consists of 496 pneumonia and 496 normal X-ray images. One of the proposed models has three main operation stages which are image pre–processing, edge detection, feature extraction and performance evaluation. First, in the Image enhancement stage, the X-ray images of patients are prepared for conversion to black and white high using different techniques and extend the small area of interest by cropping the uninteresting regions of the X-ray images and selecting the region of interest. The subsequent phase is the Image edge detection phase, the procedures involve median filtering, thresholding and edge detection techniques. Median filtering helps to eliminate salt and pepper noise which is non-linear and preserves edge information within the images. The methodology employs the practice of thresholding to high pixel values area within the region of interest. Thereafter the X-ray continues to x-ray image processing for edge detection techniques using Sobel, Robert, Major Commission, Laplacian of Gaussian (Log), and Canny edge detectors methods to obtain the edge of the image. The procedures carried out by the feature extraction stage are, erosion, dilation, border clearing, boundary encircling and feature taking out. In this stage, the objects that are not of the interest, but are present within the boundaries of the ROI, are eroded away. The boundaries of ROI are then dilated to add necessary objects to complete the boundary of ROI. The borders are cleaned up by ‘imclearborder’ and ‘bwareopen’ in order to eliminate the small residues on the edge. The boundaries are drawn with ‘bwboundary’ and the feature extraction’s value is rendered as a numerical string value.

The performance of the edge detection algorithms is assessed quantitatively using basic statistical error measures and by HVS feature-based measurement as well. The criteria used in the performance assessment include Peak Signal to noise ratio, Mean square error, Mean Absolute Error, Structural self similarity index, MS-SSIM index and Entropy. These edge detection results make known if the X-ray is for Pneumonia or non-Pneumonia subject without any mathematical information. Edge detection followed by feature extraction gives precision in the classification of pneumonia and non-pneumonia X-rays with sufficient numerical evidence. The resolution in Fig. 1 indicates the solution proposed to treat the pneumonia cases.

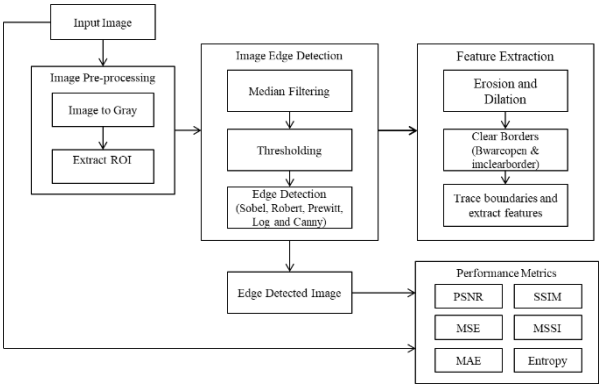

Fig. 1. Proposed Methodology

2.1 Edge Detection Techniques

2.1.1 Sobel Edge Detection

The Sobel operator utilizes a 2-D spatial gradient of an image in order to accentuate areas of space that demonstrate high frequency therefore representing an edge [13]. This approach evaluations images by measuring the gradient of intensity from each of the pixels on the image [13]. Each pixel is targeted by specifically designed kernels who are able to detect edges in the horizontal and vertical as well as solids relative to the pixel. To achieve its goal, the Sobel operator makes use of two 3 x 3 kernels of different types with the top kernel picking up the horizontal changes and the bottom kernel picking up vertical changes. These kernels are put over the original image in order to derive the estimates of the derivative. Sobel edge detection kernels are termed as:

$$M_X = \begin{bmatrix} -1 & 0 & 1 \\ -2 & 0 & 2 \\ -1 & 0 & 1 \end{bmatrix} \quad (1)$$

$$M_Y = \begin{bmatrix} -1 & 0 & 1 \\ -2 & 0 & 2 \\ -1 & 0 & 1 \end{bmatrix} \quad (2)$$

Absolute gradient in Sobel is calculated as:

$$M = \sqrt{(Mx^2 + My^2)} \quad (3)$$

2.1.2 Prewitt Edge Detection

In order to find these edges, the Prewitt operator distinguishes the strength of various edges and the angles they are oriented towards by approximating the

gradients between varying intensity pixels within the image [14]. It searches for edges in two different angles which are the horizontal and the vertical to produce one measurement of all the three angles incorporated. Also using masks or kernels of 3 x 3 sizes Kenner the Prewitt operator when on an image for upward edge detection acts like first order differential operator, yes when it contains two 3 x 3 kernels or masks. Two adjacent peeks from leaders are used to calculate the intensity difference across the edge region for several vertical edges. The vertical mask has a central column filled with zeros, that allows the focus to be mostly on these higher frequency details as opposed to the edges. In this case, the mask's middle row, which is also a zero matrix, computes these differences in reference to the original values found in the edges of the image. This procedure greatly enhances edge strength in both vertical and horizontal directions when compared to the reference image. The two masks are still based on the principle of derivative masks, which are of opposite polarity and have a zero net sum. Most significantly, the Prewitt filter is closely related to the Sobel filter. Prewitt edge detection kernels are termed as:

$$M_X = \begin{bmatrix} -1 & 0 & 1 \\ -1 & 0 & 1 \\ -1 & 0 & 1 \end{bmatrix} \quad (4)$$

$$M_Y = \begin{bmatrix} -1 & -1 & -1 \\ 0 & 0 & 0 \\ 1 & 1 & 1 \end{bmatrix} \quad (5)$$

Absolute gradient in Prewitt is calculated as:

$$M = \sqrt{(Mx^2 + My^2)} \quad (6)$$

2.1.3 Robert Edge Detection

The Roberts Cross operator performs fast and simple 2D shapes gradient imaging which does not require much computation effort [15]. This technique highlights high spatial frequency areas which correlate with edge features well. This is done in gray images through both the gray of the input and the gray of the output image. Values of pixels in the completed image show the approximate value of the absolute magnitude of spatial gradient of the image under consideration at the respective position [15]. Robert edge detection kernels are termed as:

$$M_X = \begin{bmatrix} 1 & 0 \\ 0 & -1 \end{bmatrix} \quad (7)$$

$$M_Y = \begin{bmatrix} 0 & 1 \\ -1 & 0 \end{bmatrix} \quad (8)$$

Absolute gradient in Robert is calculated as:

$$M = \sqrt{(Mx^2 + My^2)} \quad (9)$$

2.1.4 Canny's Edge Detection

The Canny edge detection algorithm is composed of many principal components that help detect a wide range of edges in an image [16]. It employs Gaussian derivative filters in order to help assess the gradient strength. This component of Gaussian value acts is helpful as it decreases the noise caused by an image. As an end result, a probable edge is simplified to single pixel wide edge lines, which means we shrink non maximum gradient magnitude's edge sections. Finally, pixels at the edges of the gradient magnitude are either kept or eliminated with the help of hysteresis thresholding. In Canny's method, there is considerable freedom to the user with three parameters: the width of the Gaussian filter which increases with image noise, and two thresholds for the hysteresis-based thresholding. The algorithm runs a 5 step process :

- Blurring: An image will go through the processes of smoothing in order to remove any noise present in the image. A Gaussian filter is employed to accomplish this function.
- Gradient detection: Eddies about the location of the edges are defined and established through the intense gradient of various gradients.
- Local maxima refinement: Only the maximal values local to the edge representation are taken to be actual edges features.
- Dual thresholding: Applications of thresholds to the edges of the image are considered a potentializing process.
- Hysteresis-based edge tracking: All the edges are finally determined and all the unconnected edges which are low units to the high prominent edges are all eliminated.

2.1.5 Laplacian of Gaussian

The Laplacian is a representation of the second spatial derivative of an image in the 2-D isotropic plane. It highlights regions where there is a rapid change in intensity a feature that is able to detect edges. The only restriction about the usage of a Laplacian is that it is prefaced with a Gaussian that is used to smoothen images. This method enhances the quality of the image by removing the high-frequency noise components during differentiation. Laplacian of Gaussian edge detection kernels are termed as:

$$M_X = \begin{bmatrix} 0 & -1 & 0 \\ -1 & 4 & -1 \\ 0 & -1 & 0 \end{bmatrix} \quad (10)$$

$$M_Y = \begin{bmatrix} -1 & -1 & -1 \\ -1 & 8 & -1 \\ -1 & -1 & -1 \end{bmatrix} \quad (11)$$

Absolute gradient in Laplacian of Gaussian is calculated as:

$$M = \sqrt{(Mx^2 + My^2)} \quad (12)$$

The SIMULINK implementation of Fig. 2 depicts Prewitt, Sobel, Log and Roberts Edge-Detection Operators, while Fig. 3 depicts the implementation of Canny Edge-Detection in SIMULINK.

Using the Gaussian noise generator, the X-ray image was purposefully controlled to be noisy, which created a noisy picture. This obtains a picture that is badly warped and even computes the picture's gradient only to the degree where existing edges exceed a certain threshold. In order to reduce the output contrast in the X-ray image, the image was 'enhanced' by the technique known as 'morphologic contrast enhancement'. In this enhancement, instead of the

central pixel, the local maximum is utilized whenever it is near the middle, else, the local minimum is employed instead. In order to allow bias and noise deny low attenuations content to penetrate the input layer, an initial median filter layer is used. It is set up that Pixels having intensity values which exceed 100 are pixels that are read as edges. A number of photographic standards are then employed which are Sobel, Robert, Prewitt, Log of Laplacian of Gaussian and called Canny edges in the Matlab code. The Simulink model parameters are as follows:

- Gaussian Gaussian noise generator mean is set as 0.
- Gaussian Gaussian noise generator variance is set as 1.
- Constant Threshold constant is set as 100.

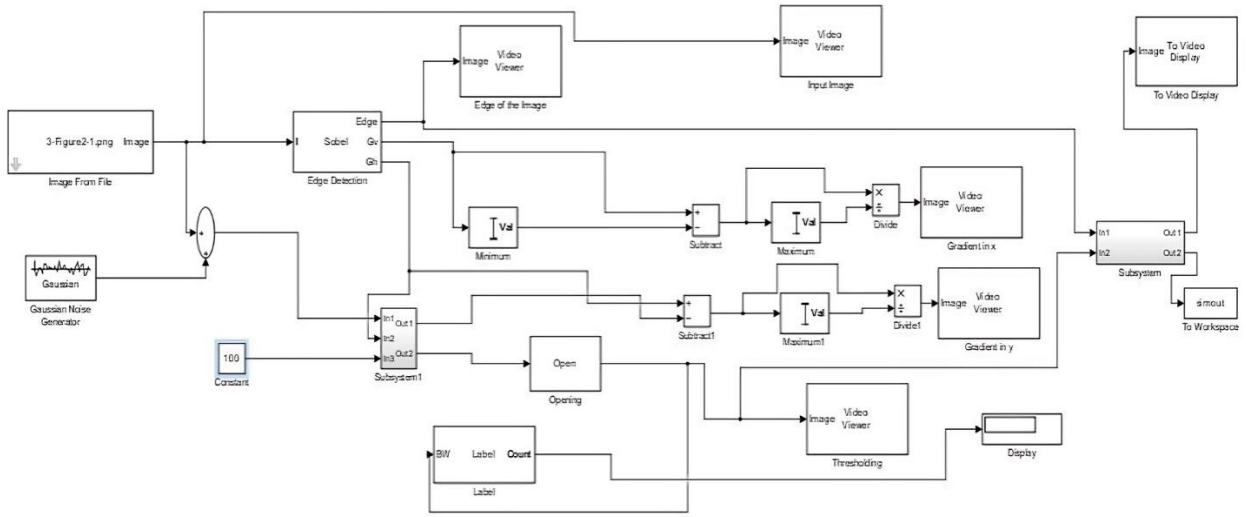

Fig. 2. Simulink Implementation of Prewitt, Sobel, Log and Robert Edge-Detection Operators

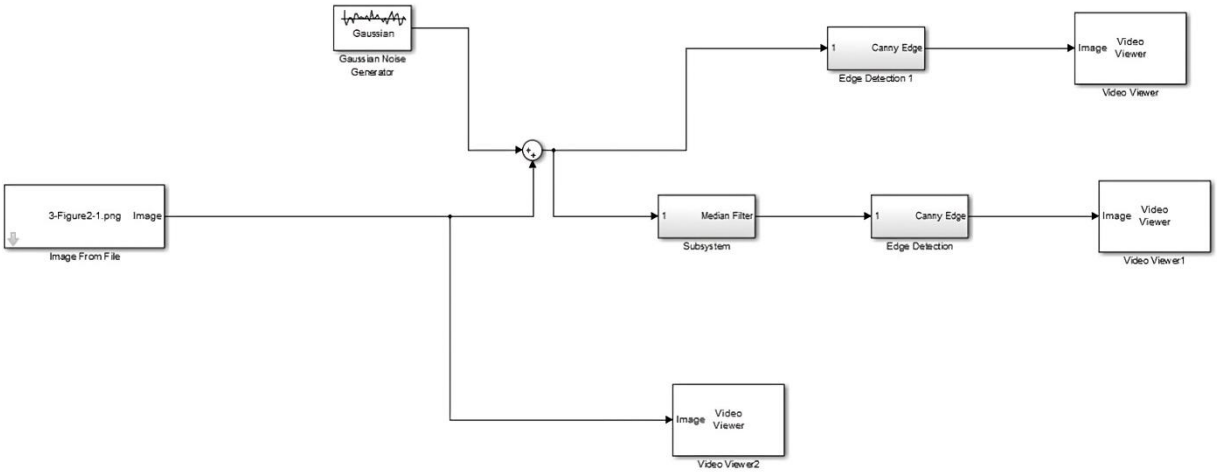

Fig. 3. Simulink Implementation of Canny Edge-Detection Operators

2.2 Performance metrics

This section provides a brief overview of image quality metrics used to evaluate the similarity and perceptual quality of X-ray images, particularly when comparing an original image to an edge-detected counterpart. The discussed metrics include both basic statistical error metrics and Human Visual System (HVS)-based measures. Table 1 presents evaluation metrics and mathematical definition.

2.2.1 Basic Statistical Error Metrics

- Mean Squared Error (MSE): Quantifies the average squared differences between pixels of two images. A lower MSE indicates better similarity.
- Peak Signal-to-Noise Ratio (PSNR): Measures the ratio between the maximum possible pixel value and the power of the noise (in decibels). Higher PSNR indicates better image quality.
- Mean Absolute Error (MAE): It is also known as Mean Absolute deviation and its a metric that works for the fine details of each pixel, as it calculates the dissimilarity of every pixel of the given images.

2.2.2 HVS Feature-Based Metrics

- Multi-Scale Structural Similarity Index (MS-SSIM): It measures how similar images are regardless of size by measuring luminance, contrast, and structure.
- Structural Similarity Index (SSIM): It uses local structures in which arrangements of H, L, and C spatially change (i.e., pixels) measure some goodness of similarity in our images: how similar an image is based on its structure and its luminance and the contrast.
- Entropy: Evaluates images on the basis of the disorder and amount of data which is present in the images' texture, the texture with a higher level of entropy is more textured.

Table 1. Evaluation metrics and mathematical definition

Metrics	Mathematical Definition	Parameters
MSE	$MSE = \frac{1}{MN}\sum_{i=1}^{M}\sum_{j=1}^{N}(x(i,j) - y(i,j))^2$	x (i, j): original X-ray image y (i, j): output image of edge detection (i,j) are the pixel position of the M×N image
PSNR	$PSNR = 10log_{10}\left(\frac{(\text{ Peak value })^2}{MSE}\right)$	peak value: maximal variation in the image data
MAE	$MAE = \frac{1}{MN}\sum_{i=1}^{M}\sum_{j=1}^{N}\lvert(x(i,j) - y(i,j))\rvert$	x (i, j): original X-ray image y (i, j): output image of edge detection (i,j) are the pixel position of the M×N image
SSIM	$SSIM = \frac{(2\bar{x}\bar{y} + C_1)(2\sigma_{xy} + C_2)}{(\hat{x}^2 + \bar{y}^2 + C_1)(\sigma_x^2 + \sigma_y^2 + C_2)}$	$\bar{x}, \bar{y}$: Mean intensities σ_x^2, σ_y^2 : Variances σ_{xy} : Covariance C_1, C_2 : Constants for stability
MS-SSIM	$MS - SSIM = \frac{1}{M}\sum_{j=1}^{M} SSIM_j$	M: Total number of windows $SSIM_j$: Structural similarity for each window
Entropy	SSIM = entropy (B)	A is the input X-Ray image B is the edge detected X-Ray image

3 Results and Discussion

The Pneumonia X-ray images with a variety of speckles, noise artifacts and resolution were utilized for examination by the proposed model. When trying to do this, extracting useful characteristics, it is of utmost importance to ensure that information is preserved and noise is reduced to the barest minimum. The researchers used a dataset described as having 496 image isolates with Pneumonia and the identical quantity without the disease. The model was able to extract X-ray feature string values. The values of string features captured are lower than 100 inspired by the pneumonia X-Rays and however greater than 100 in the non-Pneumonia X-Rays. Because the infected area of the lung is obscured, the features of X-Ray images with Pneumonia are less prominent. The lower the feature value, the severe is the infection and vice versa.

The X-Ray images are subjected to five edge detection algorithms namely Sobel, Robert, Prewitt, Laplacian of Gaussian (Log) and Canny's edge detection model. The edge detected images will have lesser number of edges detected for Pneumonia X-rays since the lung portion will be infected. The edge detected images will have more number of edges detected for non-Pneumonia X-rays since the lung portion will be less infected. The edge detection outputs provide a visual perception of whether the X-ray is of Pneumonia or non-Pneumonia without mathematical data. Edge detection technique followed by feature extraction provide an accurate classification of Pneumonia and non-Pneumonia X-rays with numerical data. The following Fig. 4 illustrates the edge detection results of test x-ray images belonging to Pneumonia class and Non-Pneumonia class. Table 2 presents a comparative analysis of quality assessment metrics for the edge-detected output images of the Pneumonia class and non-Pneumonia class.

Table 2. Quality Assessment Metrics for Edge-Detected Output Images

Xray	Feature Value	Metrics	Sobel	Robert	Prewitt	Log	Canny
 Pneumonia X-ray 1	88	PSNR	7.1542	7.1957	7.1538	7.0580	6.8479
		MSE	1.2522e+4	1.2403e+4	1.2523e+4	1.2802e+4	1.3437e+4
		MAE	100.2600	100.8705	100.2708	98.7390	93.0373
		SSIM	0.84849	0.93245	0.85102	0.68693	0.52256
		MSSIM	0.7297	0.6661	0.7300	0.8090	0.9010
		Entropy	0.0968	0.0519	0.0964	0.1879	0.4133

 Pneumonia X-ray 2	47	PSNR	5.3105	5.3313	5.3110	5.2618	5.1008
		MSE	1.9144e+4	1.9052e+4	1.9142e+4	1.9360e+4	2.0091e+4
		MAE	122.6932	123.4394	122.7019	121.0734	114.9466
		SSIM	0.79469	0.87975	0.80063	0.67646	0.50903
		MSSIM	0.7530	0.7046	0.7539	0.8089	0.8969
		Entropy	0.1243	0.0791	0.1237	0.2094	0.4442
 Non-Pneumonia X-ray 1	127	PSNR	5.2878	5.2869	5.2865	5.2941	5.3019
		MSE	1.9244e+4	1.9248e+4	1.9250e+4	1.9216e+4	1.9182e+4
		MAE	121.5871	122.4227	121.6017	119.5327	115.5043
		SSIM	0.84175	0.92043	0.84796	0.6962	0.6431
		MSSIM	0.7200	0.6624	0.7190	0.8000	0.8474
		Entropy	0.0901	0.0449	0.0899	0.1797	0.3202
 Non-Pneumonia X-ray 2	122	PSNR	5.4289	5.4236	5.4280	5.4410	5.5600
		MSE	1.8629e+4	1.8652e+4	1.8633e+4	1.8577e+4	1.8075e+4
		MAE	121.0164	121.8204	121.0351	119.0545	107.9459
		SSIM	0.87594	0.93806	0.8822	0.71659	0.46795
		MSSIM	0.6940	0.6493	0.6967	0.7886	0.9106
		Entropy	0.0803	0.0374	0.0798	0.1661	0.4813

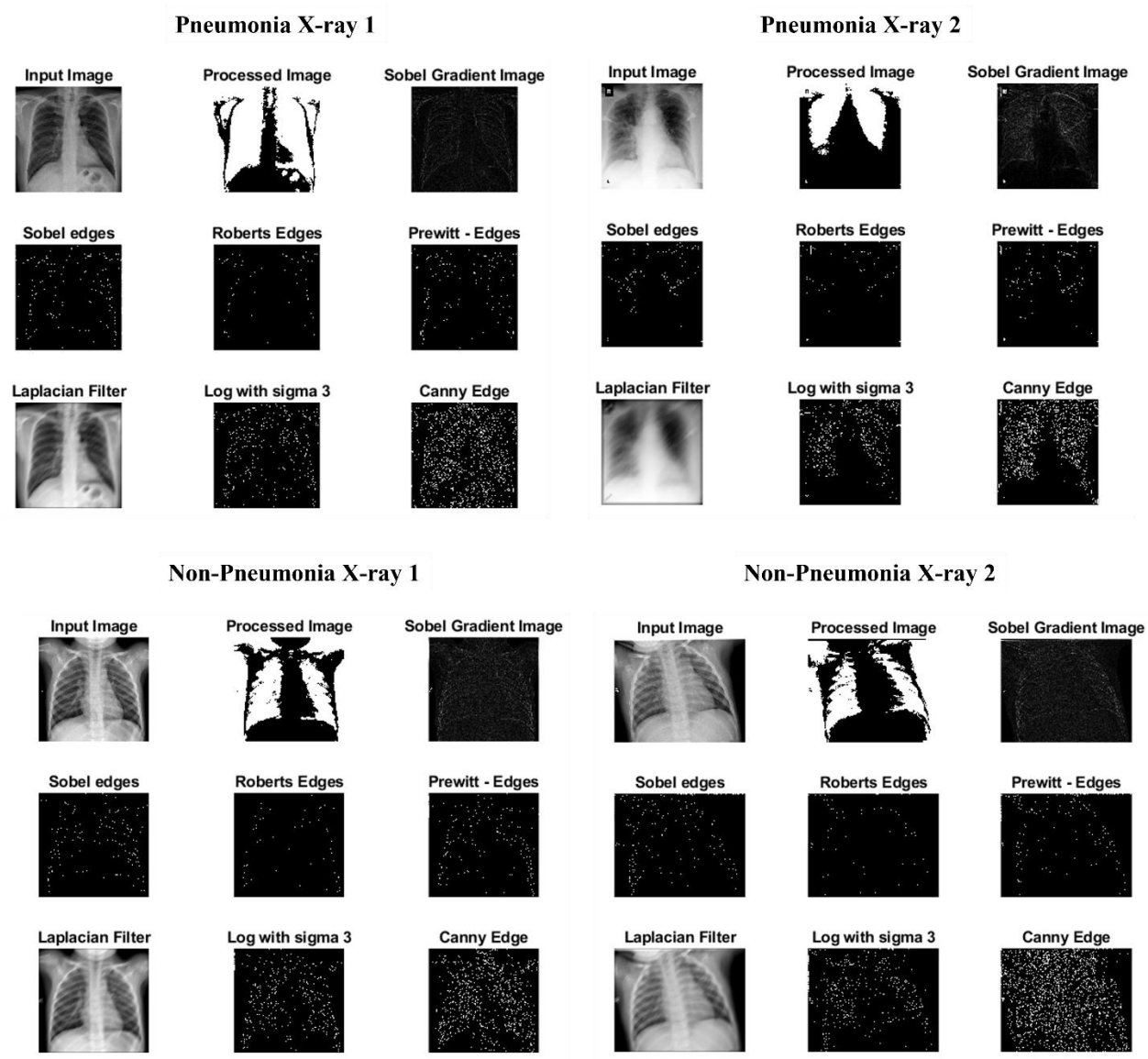

Fig. 4. Edge Detection Results of Test X-ray Images

4 Conclusion

Pneumonia testing methodologies should be developed and deployed as pneumonia has a significant global burden. The use of AI and advanced imaging techniques can enhance the diagnosis of pneumonia from chest X-rays. In this study, we presented a unique method where feature extraction was integrated with edge features for the purpose of identifying pneumonia infections from chest X-rays. The system implemented in the model employed feature extraction methods that helped determine the extent of pneumonia infection by creating determining string values that could differentiate between pneumonia X-ray images and non-pneumonia X-ray images. Among these findings, those which produced values lower than 100 were pneumonia cases and those with values more than 100 were non-pneumonia cases. For improving the detection accuracy, five algorithms for edge detection including Sobel, Robert, Prewitt, Laplacian of Gaussian and Canny's models were tested. The validation of success of the suggested model was done using various quality measure such as PSNR, MAE, MSE, MSSI, SSIM, Entropy, etc. Multiple evaluation of the image quality metrics proved the dominance of the canny edge model as compared to other edge detection models such as Sobel, Robert, Prewitt and Laplacian Of Gaussian. The outstanding performance of the Model has also been corroborated by its relatively high SSIM, MSSI and Entropy scores, thus proving its edge detection and image quality evaluation efficiency. As such, its arguments may be concluded by saying that, the Canny edge detection model stands out as the most reliable, accurate, and effective in the processes of detecting pneumonia on CXR scans.

References

1. Yee, S. L. K., & Raymond, W. J. K. (2020, September). Pneumonia diagnosis using chest X-ray images and machine learning. In *proceedings of the 2020 10th international conference on biomedical engineering and technology* (pp. 101-105). https://doi.org/10.1145/3397391.3397412
2. Lekshmy, S., Sridhar, K. P., & Roberts, M. K. (2024). Analyzing the performance of a bio-sensor integrated improved blended learning model for accurate pneumonia prediction. *Results in Engineering*, *22*, 102063.
3. Singh, S., Kumar, M., Kumar, A., Verma, B. K., Abhishek, K., & Selvarajan, S. (2024). Efficient pneumonia detection using Vision Transformers on chest X-rays. *Scientific Reports*, *14*(1), 2487. https://doi.org/10.1038/s41598-024-52703-2
4. Roy, K., Chaudhury, S. S., Burman, M., Ganguly, A., Dutta, C., Banik, S., & Banik, R. (2019, March). A Comparative study of Lung Cancer detection using supervised neural network. In *2019 international conference on opto-electronics and applied optics (Optronix)* (pp. 1-5). IEEE. doi: 10.1109/OPTRONIX.2019.8862326
5. Sanida, M. V., Sanida, T., Sideris, A., & Dasygenis, M. (2024). An advanced deep learning framework for multi-class diagnosis from chest x-ray images. *J*, *7*(1), 48-71. https://doi.org/10.3390/j7010003
6. Adithya, J., Nair, B., Aishwarya, T. S., & Nath, L. R. (2021). The plausible role of indian traditional medicine in combating corona virus (SARS-CoV 2): a mini-review. *Current Pharmaceutical Biotechnology*, *22*(7), 906-919.
7. Hwa, S. K. T., Bade, A., & Hijazi, M. A. (2020, November). Enhanced Canny edge detection for Covid-19 and pneumonia X-Ray images. In *IOP conference series: materials science and engineering* (Vol. 979, No. 1, p. 012016). IOP Publishing. https://dx.doi.org/10.1088/1757-899X/979/1/012016
8. Sahoo, T., & Pine, S. (2016, October). Design and simulation of various edge detection techniques using Matlab Simulink. In *2016 International conference on signal processing, communication, power and embedded system (SCOPES)* (pp. 1224-1228). IEEE. DOI:10.1109/SCOPES.2016.7955636
9. Ansari, M. A., Kurchaniya, D., & Dixit, M. (2017). A comprehensive analysis of image edge detection techniques. *International Journal of Multimedia and Ubiquitous Engineering*, *12*(11), 1-12. http://dx.doi.org/10.14257/ijmue.2017.12.11.01
10. Kumar, M., & Saxena, R. (2013). Algorithm and technique on various edge detection: A survey. *Signal & Image Processing*, *4*(3), 65. DOI:10.5121/SIPIJ.2013.4306
11. Makandar, A., & Halalli, B. (2015). Image enhancement techniques using highpass and lowpass filters. *International Journal of Computer Applications*, *109*(14), 12-15. DOI:10.5120/19256-0999
12. Kieu, S. T. H., Bade, A., & Hijazi, M. H. A. (2022, August). Modified canny edge detection technique for identifying endpoints. In *Journal of Physics: Conference Series* (Vol. 2314, No. 1, p. 012023). IOP Publishing. **DOI** 10.1088/1742-6596/2314/1/012023
13. Jang, W., & Lee, S. Y. (2020). Partial image encryption using format preserving encryption in image processing systems for Internet of things environment. International Journal of Distributed Sensor Networks, 16(3).
14. Fang, Y., Ma, K., Wang, Z., Lin, W., Fang, Z., & Zhai, G. (2014). No-reference quality assessment of contrast-distorted images based on natural scene statistics. *IEEE Signal Processing Letters*, *22*(7), 838-842. **DOI:** 10.1109/LSP.2014.2372333
15. Vincent, O. R., & Folorunso, O. (2009, June). A descriptive algorithm for sobel image edge detection. In *Proceedings of informing science & IT*

education conference (InSITE) (Vol. 40, pp. 97-107). https://doi.org/10.28945/3351

16. Gao, W., Zhang, X., Yang, L., & Liu, H. (2010, July). An improved Sobel edge detection. In *2010 3rd International conference on computer science and information technology* (Vol. 5, pp. 67-71). IEEE. doi: 10.1109/ICCSIT.2010.5563693
17. Malarvizhi, C., & Balamurugan, P. (2019). „Qualitative Analysis Of Various Edge Detection Techniques Applied On Cervical Herniated Spine Images.”. *ICTACT Journal of Image and Video Processing*, *9*(04), 1986-1991.